

## Capillary filling of Non-Newtonian fluids

Md Ashker Ibney Rashid<sup>1</sup>, Shadi Ansari<sup>1</sup>, Prashant R. Waghmare<sup>2</sup>, David Nobes<sup>2,\*</sup>

<sup>1</sup>Department of Mechanical Engineering, University of Alberta, Edmonton, Canada

<sup>2</sup>Faculty of Mechanical Engineering, University of Alberta, Edmonton, Canada

\*corresponding author: dnobes@ualberta.ca

---

**Abstract** Non-mechanical pumping in microfluidic devices has emerged as a promising option for the pumping of biomolecules. Capillary filling due to dominant surface forces at the micro-scale is one such non-mechanical pumping approach. The ability of the pumping due to the capillary filling process is dictated by the surface energy of the channel surface and the physical properties of the liquid. The primary limitation for such surface tension driven flow is the induced drag caused by the inherent viscosity of the liquid and to determine the magnitude of this drag force, due to viscous drag, knowledge of velocity profile across the channel is of utmost priority. The capillary imbibition process is an intrinsically transient process and in this study the commonly adopted notion of fully developed velocity profile is experimentally verified. In such flows three different regimes along the flow can be found, i.e., surface forces dominant regime—behind the air-liquid interface, developing flow regime—where the viscous forces and surface forces are comparable to each other, and the developed regime—where the viscosity dictates the flow dynamics. In this study three different regimes along the microchannel (developing, developed and behind the liquid-air interface) for Newtonian and non-Newtonian liquid are studied, using micro-particle image velocimetry ( $\mu$ PIV). It is evident that, in the surface tension dominant regime the velocity near the wall region is the maximum as opposed to the developed regime where the velocity at the center of the channel is maximum. The shifting of the maximum velocity location from near wall region to center of the channel resembles conventional pressure driven flow dynamics. Nonetheless, in the case of the capillary imbibition process, the center line velocity never attains a constant magnitude. The obtained results allowed the determination of different length and time scales for three different regimes. A propose simplified theory for entrance length, in the case of capillary filling, suggests that the entrance length is exclusively dependent on the Ohnesorge number (ratio between the viscous to surface tension force) and the wettability of the surface. The entrance length i.e., the distance from the inlet of the channel at which the velocity profile attains the developed velocity profile is also determined from the experimental results and is further compared with the theoretically proposed correlation. The fluid with different viscosities and surface tension is used to change the magnitude of viscous and surface forces. This set of results is validated against the proposed correlation for entrance length. It is the ultimate aim of this study is to propose a simple mechanism for the measurement of viscosity for a liquid using the velocity profile information. This is crucial for complex liquid particularly for non-Newtonian fluids where the conventional rheological measurements are not only time consuming but also requires state-of-the-art facility to obtain the measurements.

**Keywords:** Capillary driven flow, Non-Newtonian flow, PIV

---

### 1 Introduction

Theoretical analysis of capillary process has been well studied and understood [1] [2]. The autonomous pumping ability allowed capillary filling process as a promising option as a passive pumping in microfluidic devices [3]. Capillary pumping is also used to design cooling system in electronic packaging [4] and delivery system of  $\mu$ -TAS (micro total analysis system) in the area of medicine and biology [5] and to produce nanowires and nanorods in microfabrication designs [6][7]. From theoretical point of view capillary filling process is due to the abundance of the surface forces or the surface energy and wettability of the substrate. The ability or pumping power of this autonomous pumping is mainly dictated by the physical and interfacial properties. Several theoretical approaches have been developed so far to predict the imbibition of liquid due to capillary action. In general the driving force is balanced against the resistive force which is the viscous drag due to the inherent physical properties of the liquid. The knowledge of the velocity profile across the channel is an utmost requirement to quantify this viscous drag. In most of the cases the fully developed velocity profile is assumed to obtain the magnitude of the viscous drag. In this study, the assumption of fully developed velocity profile is verified against the experimental observation. The experimental analysis is further extended for non-Newtonian fluids and the velocity profile development in such cases is analyzed experimentally.

Capillary filling of non-Newtonian fluid is one of the complicated scenarios. Whether the case is underfilling of epoxy encapsulant in electronic packaging [8], blood flow [10] or the viscoelastic flow through porous media [9]. In such scenarios fluid is non-Newtonian and shear dependent viscosity plays a major role in the capillary filling process. Since most of the fluids used in practice has a non-Newtonian characteristics such as blood, polymeric solution, DNA in such cases the functional relationship between viscosity and capillary filling needs to be understood.

In this paper the capillary filling of non-Newtonian fluid is analyzed experimentally and results are compared with the traditional theoretical model. The objective of this paper is to examine the capillary filling process for both Newtonian and non-Newtonian fluid in square shaped vertically aligned capillary channel. So far, Capillary filling of only power law fluid has been studied experimentally [12] and analytically [13]. But the comparison between the experiential results and analytical model has not been studied in detail [11].

## 2 Experimental setup

Fig.1 shows the experimental setup which was developed to capture the velocity profile across the channel during the imbibition of liquid due to capillary action. A square glass tubing (VitreTubes™, Vendor: VitroCom, Product No.8240) was used as a capillary of  $400\mu\text{m} \times 400\mu\text{m}$  and length of 8cm. The special holder was designed to hold the capillary in perfectly vertical orientation. The liquid reservoir was placed underneath the capillary and reservoir level was adjusted using knob of the adjustable-height table. The liquid reservoir was brought in contact with the bottom of the capillary by turning the knob very slowly so that the imbibition of liquid is merely due to the capillary action. The field of view for the camera (Phantom V711, Vision Research, Ametek,Inc.) was set at 2cm from the bottom of the microchannel, to avoid the entrance effect. The camera was carefully focused at proportionate plane across capillary i.e., approximately in between the front and back wall. A light source (Fiber light, MI-152) was used in line with the view of the camera with back light illumination arrangement.

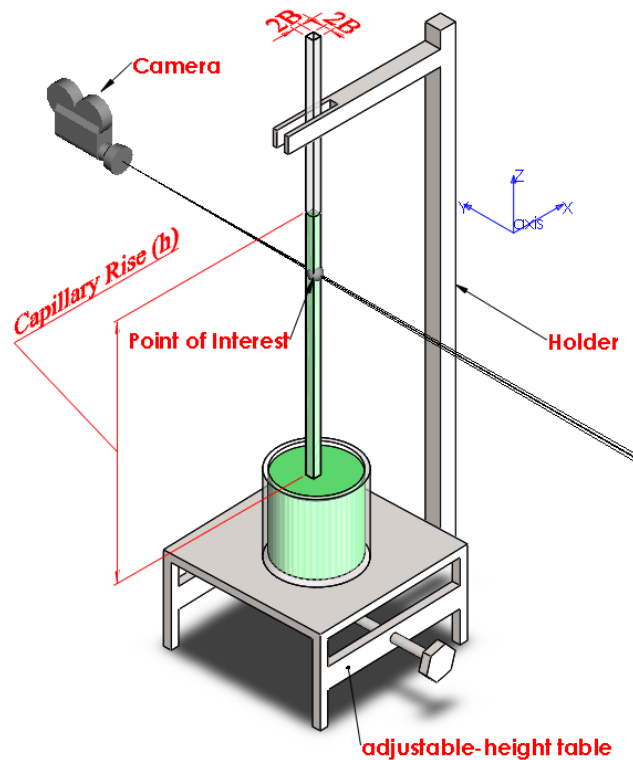


Fig. 1 Setup of the experiment

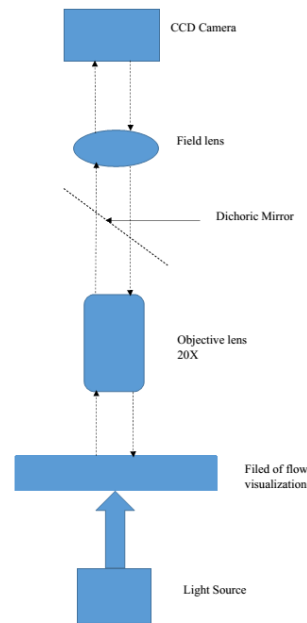


Fig. 2 Schematic of the PIV setup

Water was used as the Newtonian fluid whereas polyacrylamide-water solution was considered as a non-Newtonian fluid. Polyacrylamide solution was prepared using granular polyacrylamide powder of bulk density  $0.7\text{gmcm}^{-3}$  and particle size  $1000\mu\text{m}$ . Powder was slowly added in 100ml of DI water to get 0.1% concentration of the solution. To mix up the solution a magnetic stirrer was used with 100rpm for 3 hours [14]. Non-Newtonian parameter of this solution was measured using a double gap cylinder type rheometer (RheolabQc). The Power law index was measured  $n = 0.44$  and consistency index was measured  $m = 0.28$ . Fluorescent particles (Fluoro-Max<sup>TM</sup>, CAT.No R0200) of  $2\mu\text{m}$  of diameter was used as tracer particles. The image was captured using the PIV setup whose schematic diagram is shown in Fig.2 [15]. In the case of water as a test fluid, the images were captured with 18000 fps (frame per second) whereas for polyacrylamide solution fps was 1300. An infinity corrected objective lens of 20X was used to obtain the field of view of  $550\mu\text{m} \times 480\mu\text{m}$ .

### 3 Image-Processing

A commercial image processing software (Davis 8.2, LaVision GmbH.) was used to do the PIV processing. At first step image was inverted with an appropriate scale to get brighter image of the particle. A geometric mask was defined to reduce the background noise and get the fully developed flow region in the processing field of view. For vector calculation sequential cross correlation method is used with multi pass decreasing size iterations. For first pass the window size was  $96 \times 96$  with 50% overlap and for second pass the window size was  $64 \times 64$  with 87% overlap. Processed vector files were then used by a commercial software package (Matlab2014a) for plotting velocity profile and calculating average centerline velocity. Average centerline velocity was calculated by averaging all the velocity vector in a  $3 \times 3$  area in the center for each frame of image.

### 4 Results

Capillary filling for Newtonian fluid is analyzed both experimentally and theoretically during the traveling of the water-air interface along the field of view. Fig.3 shows the development of flow field behind the moving interface and subsequent changes in the trailing velocity field is presented from six different time steps. A color map represents the scale of the velocity vector. Fig.3(a) shows the flow field at time  $t = 8.2\text{ms}$  and Fig.3(b)-(f) show subsequent flow field with time difference of 4.1ms. In Fig.3(a) maximum velocity is observed at three

phase contact line, i.e., near the wall region. This is due to no slip condition at the wall to free slip condition at the contact surface. It is to be noted that for theoretical modeling approaches the velocity profile is assumed to be parabolic shape velocity profile. From raw data as well as from Fig.3(a)-(f) it was evident that the shape of the meniscus remained unaltered during the transport, hence one can conclude that the variations in the dynamic contact angles can be neglected. From Fig.3(c)-(e) it is evident the maximum velocity regime is shifted from near wall to the center of the channel.

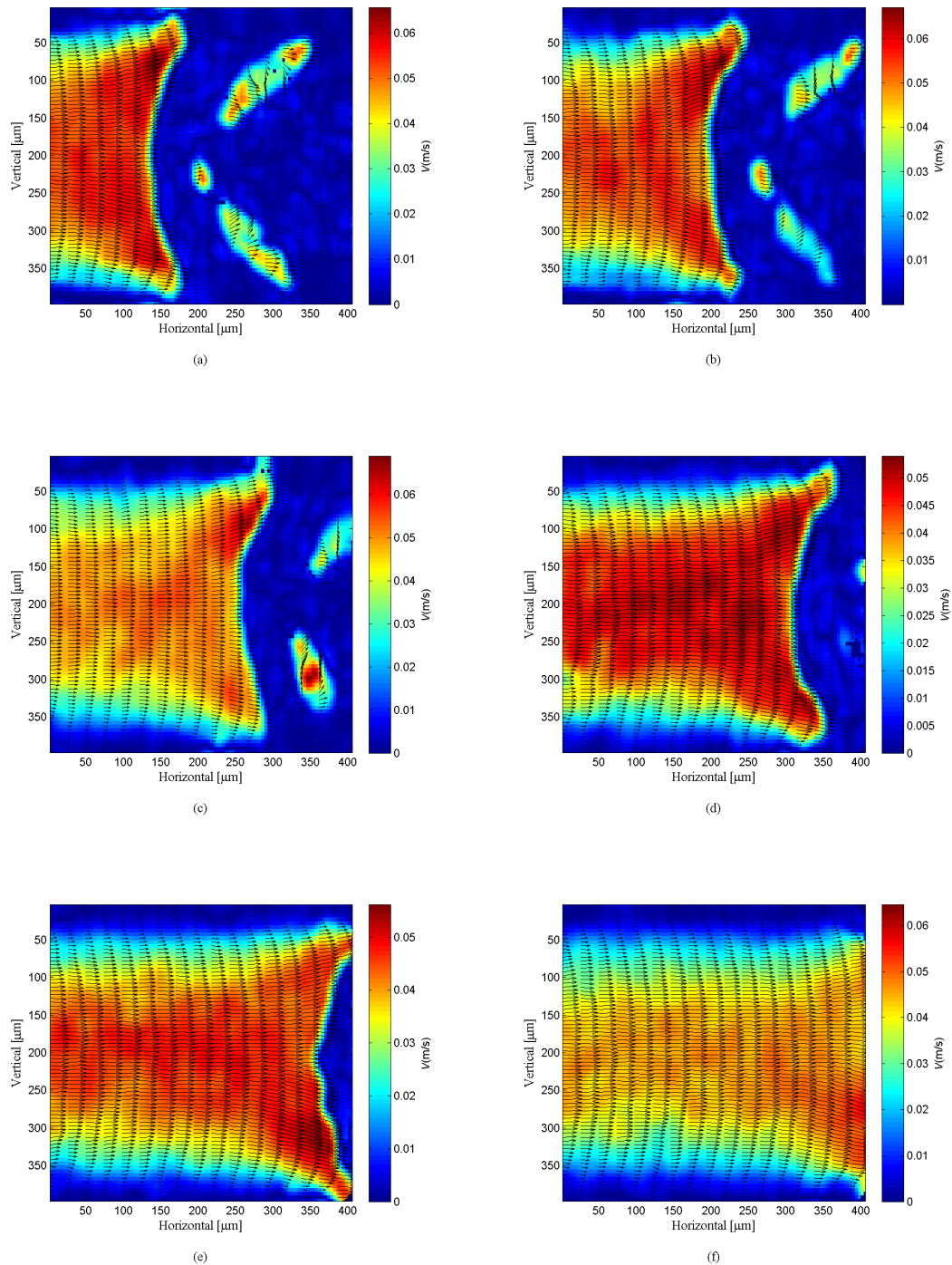


Fig. 3 Velocity profile of water at time (a)  $t = 8.2\text{ms}$ , (b)  $t = 12.3\text{ms}$ , (c)  $t = 16.4\text{ms}$ , (d)  $t = 20.5\text{ms}$ , (e)  $t = 24.6\text{ms}$ , (f)  $t = 28.7\text{ms}$

In the case of non-Newtonian fluid (polyacrylamide solution), we get similar kind of result which is shown in Fig.4. The shape of meniscus was not symmetric. The raw data suggests the presence of precursor film for non-Newtonian fluid which was not observed in the case of water. Moreover, the shape of the interface was different during the imbibition process. The analysis of three phase contact line of non-Newtonian fluid needs to be studied in greater detail to comment on such observation. The change in the surface tension magnitude (for polyacrylamide solution the surface tension magnitude was measured using pendant drop as 50mN/m and contact angle was approximately the same as water which is 7°). Fig.4(a)-(e) show subsequent flow field with time difference of 30.6ms.

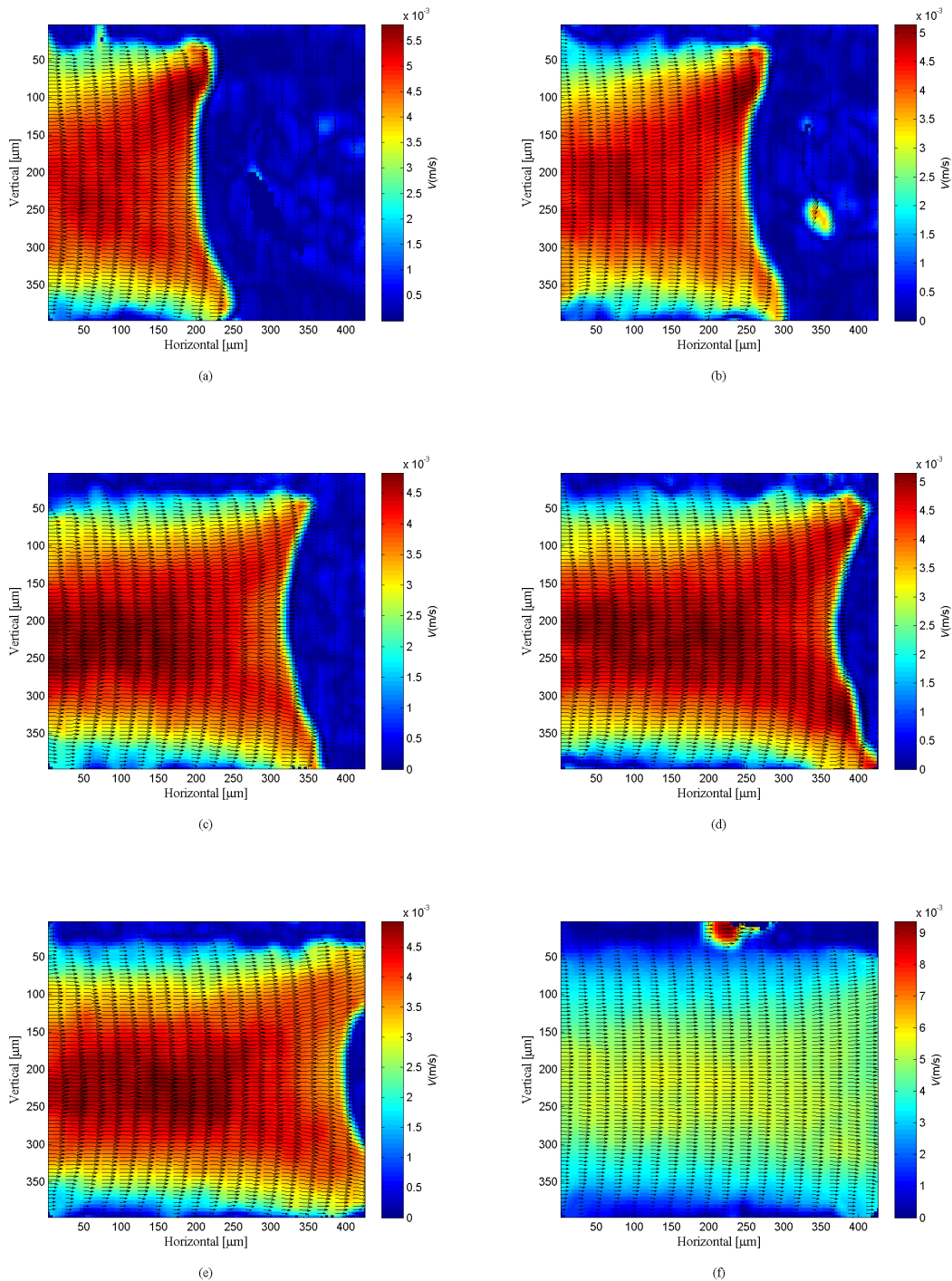


Fig. 4 Velocity profile of Polyacrylamide solution at time (a)  $t = 83.1\text{ms}$ , (b)  $t = 113.8\text{ms}$ , (c)  $t = 152.3\text{ms}$ , (d)  $t = 183.1\text{ms}$ , (e)  $t = 213.5\text{ms}$ , (f)  $t = 242.3\text{ms}$

It is evident that the development in the velocity profile is similar for Newtonian and non-Newtonian case. In most of the theoretical approaches the velocity profile is assumed to be fully developed velocity profile which is further used to determine the viscous force. Hence experimental result is used to validate this assumption.

#### 4.1 Theoretical prediction of velocity profile

A theoretical model is developed for capillary rise of non-Newtonian fluid in a microchannel with a square shape cross section[16]. The position of the origin is at the intersection with centerline of the microchannel and top surface of the fluid in the reservoir [16]. Here the capillary rise is defined as the distance between the origin and the lowest peak of the meniscus. Conservation of momentum is the basis for this theoretical model. Fluid is assumed to be homogeneous, non-Newtonian and incompressible. For a control volume of fluid present inside the capillary of side length  $2B$  the conservation of momentum along  $z$  direction can be written as[17];

$$\sum F_z = \frac{\partial}{\partial t} \left[ \int_0^h \int_{-B}^B \int_{-B}^B \rho v_z dx dy dz \right] + \int_{-B}^B \int_{-B}^B v_z (-\rho v_z) dx dy \quad (1)$$

In the case of non-Newtonian fluid, the power law model is used. For power law fluid

$$\begin{aligned} \tau &= m \left( \frac{dv_z}{dx} \right)^n \\ \mu_{eff} &= m \left( \frac{dv_z}{dx} \right)^{n-1} \end{aligned}$$

here  $m$  is the consistency index and  $n$  is the power law index. For this model it is assumed that flow attains fully developed velocity instantly and for  $v_z$  (fully developed velocity profile), flow between parallel plates will be used. For power law fluid the fully developed velocity profile is

$$v_z = \frac{3}{2} \frac{dh}{dt} \left[ 1 - \left( \frac{x}{B} \right)^{\frac{n+1}{n}} \right] \quad (2)$$

where  $\frac{dh}{dt}$  is the displacement rate of the flow front. As no external forces is considered for this model  $\sum F_z$  (summation of all forces considered for this modeling) consists of five different forces that act on the control volume along  $z$  direction. Which are viscous force ( $F_v$ ), pressure force at the flow front ( $F_{pf}$ ), pressure force at the inlet ( $F_{pi}$ ), gravity force ( $F_g$ ) and surface tension force ( $F_s$ ). For fully developed flow the viscous force can be determined as [17]

$$F_v = 4 \int_0^h \int_{-B}^B \left( m \left( \frac{dv_z}{dx} \right)^n \right)_{x=\pm B} dx dz = 8m \left( \frac{3n+3}{2Bn} \right)^n \left( \frac{dh}{dt} \right)^n \quad (3)$$

The detailed analysis of theoretical modeling and details of pressure force at the inlet of the channel, gravity force and surface tension force can be found elsewhere [17]. The pressure field at the inlet of the channel for non-Newtonian fluid can be expressed as[17][18].

$$p(x, y, 0) = P_o - \left[ 1.11\rho B \frac{d^2h}{dt^2} + 1.158\rho \left( \frac{dh}{dt} \right)^2 + \frac{1.772}{B} m \left( \frac{3n+3}{2Bn} \right)^{n-1} \left( \frac{dh}{dt} \right)^n \right] \quad (4)$$

Using Equations 2-4 and forces defined earlier one can obtain the Equation 1 in the form of differential equation which can be solved using Runge-Kutta 4th order method to obtain the transient variation in the penetration depth,  $h$ . The obtained differential equation is

$$8m \left( \frac{3n+3}{2Bn} \right)^n \left( \frac{dh}{dt} \right)^n + 4B\sigma (\cos \theta_d - 1) + 4.44B\rho B^2 \frac{d^2h}{dt^2} + 4.632\rho B^2 \left( \frac{dh}{dt} \right)^2 + \frac{1.772m}{B} \left( \frac{3n+3}{2Bn} \right)^{n-1} \left( \frac{dh}{dt} \right)^n - 4B^2 h \rho g + 4B\sigma \cos \theta_d = 6\rho B^2 \left( \frac{n+1}{2n+1} \right) \left( h \frac{d^2h}{dt^2} + \left( \frac{dh}{dt} \right)^2 \right) - 9\rho B^2 \left( 1 - \frac{2n}{2n+1} + \frac{n}{3n+2} \right) \left( \frac{dh}{dt} \right)^2 \quad (5)$$

where  $\sigma$  is the surface tension,  $\cos \theta_d$  is the dynamic contact angle,  $\rho$  is the density of the fluid and  $g$  is the gravitational acceleration.

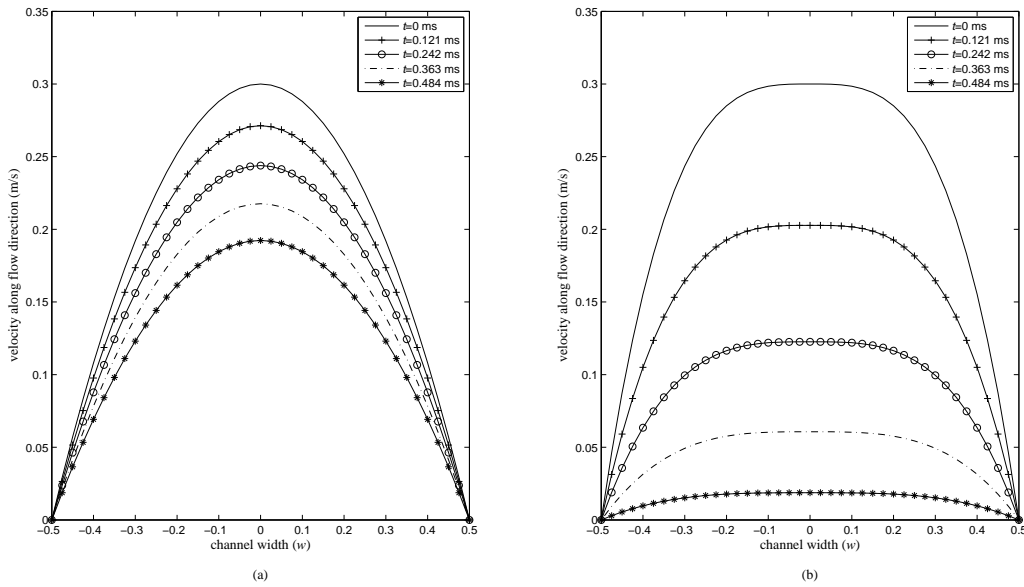


Fig. 5 Fully developed velocity profile at different time step for (a) water and (b) polyacrylamide solution from theoretical modeling

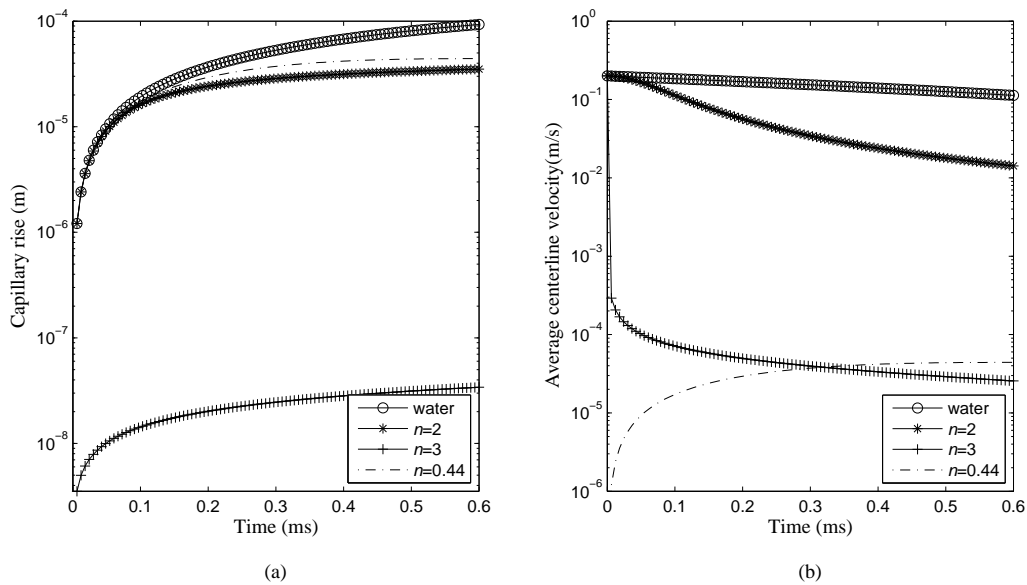


Fig. 6 (a) Capillary rise and (b) Average centerline velocity as a function of time

Fig.5 shows the difference between the shape of velocity profile for Newtonian and non-Newtonian fluid at different time step. The fully developed velocity profile for water across the channel width is presented in Fig.5(a) where the assumption of fully developed velocity profile reflected in the shape of the velocity profile. In the case of the capillary filling process as the flow progresses the resistance to flow due to viscous drag and gravity increases which in turn retards the transport. Therefore, the decrement in the centerline velocity can be observed as presented in Fig.5(a)

In the case of non-Newtonian fluid, as presented in Fig.5(b), the shear thinning nature of liquid flattened the velocity profile across the channel. As observed in the case of Newtonian fluid, in case of non-Newtonian fluid also the centerline velocity retards with respect to time. Compared to the Newtonian fluid, a symmetric curved velocity profile with a flat portion in the center is observed for non-Newtonian fluid. This velocity profile is observed due to shear thinning characteristics of the fluid. Near the wall, due to induced shear stress the viscosity is higher than in the center of the channel. Although the flat portion of the velocity profile remained same in the subsequent profiles the centerline velocity decreased with time. In comparison with the Newtonian fluid the decreasing rate of the centerline velocity for non-Newtonian fluid, is much faster.

In Fig.6(a) we can observe the capillary rise as function of time for different fluid. For different kind of liquids the capillary rise increases asymptotically and eventually attains the equilibrium height. It is evident that shear thinning fluid reaches equilibrium height much quicker as compared to the shear thickening fluid. It is due to the fact that the shear thinning fluid travels faster due to decreased viscosity. In the case of centerline velocity as depicted in Fig.6(b) for shear thinning fluid it increases asymptotically due to decrement in viscosity from induced shear stress from the wall. The centerline velocity from experimentally observed results is compared with the theoretically observed variations.

Fig.7 shows the centerline velocity from experimental results. Although the magnitude of the centerline velocity is different from theoretical model, the obtained results followed the proposed theory. It is to be noted that the theoretical model is developed based on the fully developed velocity. Moreover, the velocity profile considered in this analysis assumes the width of channel is very small compared to the depth of the channel. Ideally for square capillaries double parabolic profile needs to be considered.

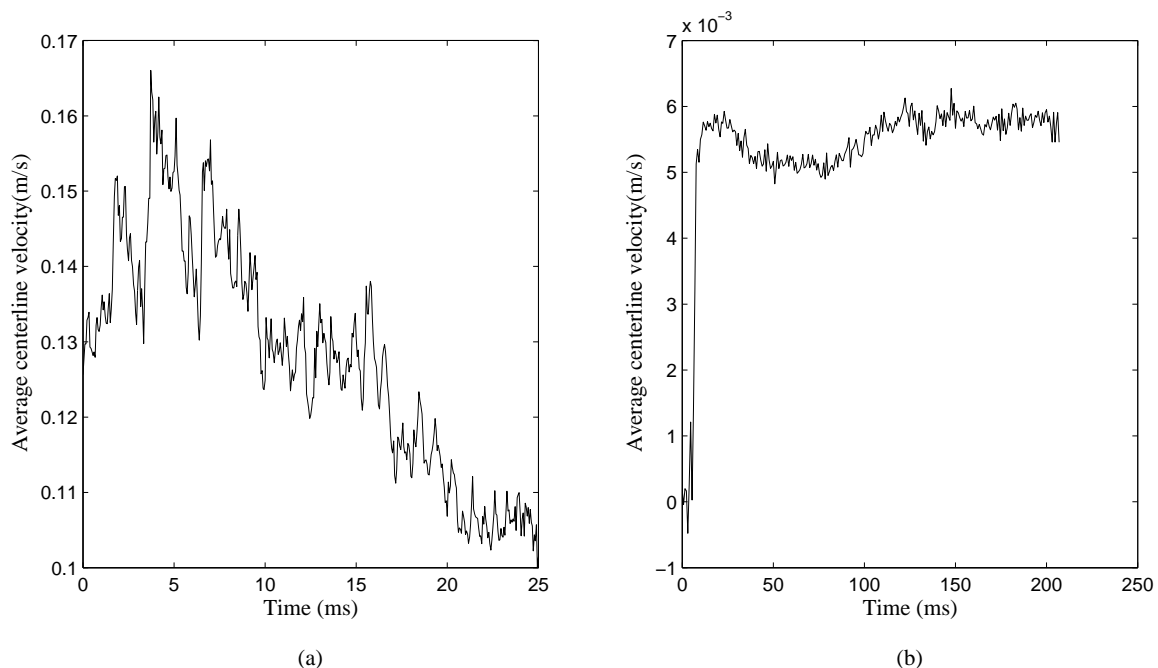


Fig. 7 Average centerline velocity with time for (a) water and (b) polyacrylamide solution



## 5 Conclusion

The capillary filling process in a vertical channel is analyzed experimentally and compared with the theoretical model. Effect of non-Newtonian fluid in capillary filling process was rectified. From the theoretical modeling and experimental results it is observed that shear thinning fluid reaches the fully developed velocity profile faster than any Newtonian or shear thickening fluid. As the shape of velocity profile is dependent on viscosity, an empirical model can be developed from experimental result to measure the viscosity of the fluid. For further development of theoretical modeling some assumptions about the flow needs to be understood more precisely.

## Acknowledgment

The authors gratefully acknowledge financial support from Natural Sciences and Engineering Research Council (NSERC) of Canada, the Alberta Ingenuity Fund, and the Canadian Foundation for Innovation (CFI).

## References

- [1] Washburn E(1921) The dynamics of capillary flow. *Physical Review*, vol.17, pp 273-283. doi: 10.1103/PhysRev.17.273
- [2] Lucas R (1918) Ueber das Zeitgesetz des kapillaren Aufstiegs von Flüssigkeiten. *Kolloid-Zeitschrift*, vol.23, pp 15-22. doi: 10.1007/BF01461107
- [3] Zimmermann M, Schmid H, Hunziker P, Delamarche E (2007) Capillary pumps for autonomous capillary systems. *Lab on a Chip*, vol.7, pp 119-125.
- [4] Wajman T (2009) Analysis and design of capillary pumps for applications in electronic components cooling systems. *Zeszyty Naukowe Politechniki Lodzkiej Elektryka*, pp 63-68.
- [5] Ahn JJ, Oh JG, Choi B (2004) A novel type of a microfluidic system using ferrofluids for an application of  $\mu$ -TAS. *Microsystem Technologies-Micro and Nanosystems-Information Storage and Processing Systems*, vol.10, pp 622-627. doi:10.1007/s00542-003-0340-9
- [6] Cao L, Chen Hong-Z, Li Han-Y, Zhou Han-B, Sun Jing-Z, Zhang Xiao-B, Wang M (2003) Fabrication of rare-earth biphthalocyanine encapsulated by carbon nanotubes using a capillary filling method. *Chemistry of materials*, vol.15, pp 3247-3249.
- [7] Kiang Ching-H, Choi Jong-S, Tran T T, Bacher A D (1999) Molecular Nanowires of 1 nm Diameter from Capillary Filling of Single-Walled Carbon Nanotubes. *The Journal of Physical Chemistry B*, vol.103, pp 7449-7451. doi: 10.1021/jp991424m
- [8] Young Wen-B (2011) Non-Newtonian Flow Formulation of the Underfill Process in Flip-Chip Packaging. *IEEE Transactions on Components Packaging and Manufacturing Technology*, vol.1, pp 2033-2037. doi:10.1109/TCPMT.2011.2169260
- [9] Galindo-Rosales F J, Campo-Deano L, Pinho F T, Van B E, Hamersma P J, Oliveira M S N, Alves M A Microfluidic systems for the analysis of viscoelastic fluid flow phenomena in porous media. *Microfluidics and Nanofluidics*, vol.12, pp 485-498. doi:10.1007/s10404-011-0890-6
- [10] Cito S, Ahn Yeh-C, Pallares J, Duarte R, Chen Z, Madou M, Katakis I Visualization and measurement of capillary-driven blood flow using spectral domain optical coherence tomography. *Microfluidics and Nanofluidics*, vol.13.2, pp 227-237. doi: 10.1007/s10404-012-0950-6
- [11] Berli C L A, Urteaga R(2014) Asymmetric capillary filling of non-Newtonian power law fluids. *Microfluidics and Nanofluidics*, vol.17, pp 1079-1084. doi:10.1007/s10404-014-1388-9
- [12] Srivastava N, Burns MA (2006) Analysis of non-Newtonian liquids using a microfluidic capillary viscometer. *Analytical Chemistry*, vol.78, pp 1690-1696. doi:10.1021/ac0518046
- [13] Digilov R M (2008) Capillary Rise of a Non-Newtonian Power Law Liquid: Impact of the Fluid Rheology and Dynamic Contact Angle. *LANGMUIR*, vol.24, pp 13663-13667. doi:10.1021/la801807j

- [14] Ansari S, Rashid MAI, Chatterjee O, Waghmare P R, Ma Y, Nobes D S (2015). Visualization of the viscous effects of non-Newtonian fluids flowing in mini-channels. In: Proceeding of the 10th, Pacific Symposium on Flow Visualization and Image Processing
- [15] Sen D, Nobes D S, Mitra S K(2012) Optical Measurement of pore scale velocity field inside micro porous media. *Microfluidics Nanofluidics*, vol.12, pp 189-200.
- [16] Xiao Y, Yang F, Pitchumani R(2006) A generalized analysis of capillary flows in channels . *Journal of Colloid and Interface Science*, vol.298, pp 880-888.
- [17] Dreyer M, Delgado A, Path H J(1994) Capillary Rise of Liquid between Parallel Plates under Microgravity. *Journal of Colloid and Interface Science*, vol.163, pp 158-168. doi:<http://dx.doi.org/10.1006/jcis.1994.1092>
- [18] Levine S, Reed P, Watson E J (1976) Adsorption,Catalysis,Solid surfaces,Wetting,Surface Tension and Water. In: Marker (ed) *Colloid and Interface Science*, Vol.III. Academic press, New York, pp 403